Pertanika J. Sci. & Technol. 25 (1): 293 - 302 (2017)

PERTANIKA JOURNALS

SCIENCE & TECHNOLOGY

Journal homepage: http://www.pertanika.upm.edu.my/

Yawing Force of Electric Trimmers of a Hybrid Buoyant Aerial Vehicle

Haque, A. U.[1], Asrar, W.[1]*, Omar, A. A.[2], Sulaeman, E.[1] and Ali, J. S. M.[1]

[1] *Department of Mechanical Engineering, International Islamic University Malaysia, 50728 IIUM, Kuala Lumpur, Malaysia*

[2] *Department of Aeronautical Engineering, University Of Tripoli, 13154, Tripoli, Libya*

ABSTRACT

All buoyant and hybrid buoyant aerial vehicles have directional stability issues at low speed. Electric trimmers are one of the potential solutions for controlling the yaw motion of such vehicles in which partial lift is obtained from the wings. However, available propeller disk area of such trimmers is limited due to small surface area of the vertical tail. In the present work, maximum input power required by thin electric propellers with different pitch values are compared to obtain an optimised value of pitch for propeller selection. Analytical as well as computational techniques are employed to evaluate the moment generated by tangential thrust produced by a ducted propeller. *Motocalc*® software under predicts the thrust value when compared with the computational results under the same flow conditions. The estimated yaw force produced by the propeller is quite significant and it can also be used for creating differential thrust using twin electric motors.

Keywords: Advance Ratio, Computational Fluid Dynamics, Hybrid Buoyant Aerial Vehicle, Static Thrust, Turning, Thin Electric Propeller

INTRODUCTION

Airships are directionally unstable (Khoury & Gillett (1999; Carichner & Nicolai, 2013)) and little information is available on the stability of hybrid buoyant airships in yaw. In a recent experimental study by Andan, Asrar & Omar (2012) on a generic model of a hybrid airship, it was found that such a vehicle is marginally stable in yaw. Such response can cause poor manoeuvrability, especially at low speeds. The yaw/turning performance of a hybrid buoyant aerial vehicle can be enhanced by inserting an electric fan in the lower vertical tail or at the nose of the hull (Haque et al.,

Article history:
Received: 08 January 2016
Accepted: 11 November 2016

E-mail addresses:
anwar.haque@live.iium.edu.my (Haque, A. U.),
waqar@iium.edu.my (Asrar, W.),
aao@aerodept.edu.ly (Omar, A. A.),
esulaeman@iium.edu.my (Sulaeman, E.),
jaffar@iium.edu.my (Ali, J. S. M.)
*Corresponding Author

ISSN: 0128-7680

2014). This concept is perhaps similar to that used in traditional advertising blimps for circuit flight over a fixed location (Stockbridge et al., 2012). Direct current (*DC)* brushless motor generates the required thrust which can be manipulated as the yaw force when installed in a plane perpendicular to the incoming air.

For small blimps, the yaw is produced by using *DC* electric motors placed close to the gondola at the base of the hull. Such motors are usually ducted with the help of a metallic ring to meet safety requirements. The moment arm of such motors is quite small as the location of installation is close to the centre of gravity *(CG).* There have been many studies carried out in the area of dynamic stability of buoyant and hybrid buoyant aerial vehicles; however, information regarding the yawing response and yaw force generated by the electric thrusters is quite limited. In the present work, an analytical and computational effort is made to fill this gap. A generic model of a hybrid buoyant aerial vehicle *(HBAV)* designed by (Andan, et al*.,* 2012) is taken as a test case in which an electric propeller is used to obtain the performance parameters of an electric propeller. In order to generate the yaw force, electric trimmers are placed in a direction perpendicular to the free stream velocity.

Usually, three types of control surfaces are required to manoeuvre an aircraft i.e. *Elevators* to control the Pitch, *Rudders* to control the Yaw and *Ailerons* to control the Roll. In the case of airships as well, it is conventional to use rudders to control the yawing motion. However, rudders can be replaced by generating a differential thrust with the help of electric motors. In this way, if there is a yaw signal, the speed of the electric motors not only depends on the throttle signal but on both throttle and yaw signals. In this case, the speed of second motor set is decreased or increased compared with the first motor set, as per the requirement to either decrease or increase the yaw. This is discussed in detail in the section on result and discussion.

The term thrust is always used for the estimation of the propulsive force generated by a propeller in the forward flight, which is in fact the required yaw force to trim the vehicle as done by rudders in the case of aircraft (Schroijen, et al*.,* 2008). Similar to the helicopter rotor, the flow around such a propeller is heavily distorted and massive flow separation occurs at its tip. For hybrid buoyant aerial vehicles, such effects and losses can be minimised to some extent by placing the propeller blades inside the lower vertical tail of a+ *type* empennage arrangement. Also, similar to the wing of an aircraft, a propeller has its own airfoils, which can have an aerodynamic as well as a geometric twist. This airfoil creates pressure difference between its windward and leeward side. In order to estimate its pressure difference, the aerodynamic characteristics of the individual airfoil must be known.

In this paper, various propeller combinations are evaluated using a brushless *DC* motor as the propulsion system. The choice of a brushless DC motor is due to its better performance and comparatively high operating efficiencies compared with brushed *DC* motors. There are many different types of propellers, such as fixed-pitched, ground-adjustable, two-position, controllable, automatic, constant speed, feathering constant speed and reverse pitch; out of these, fixed pitch is selected as it does not allow for any change in blade angles and is usually available as a single piece. The available thrust is calculated using *MotoCalc*® software, which is an open source code usually used for R/C airplane's propulsion system sizing and analysis. It has a large database of electric motors, batteries and speed controllers (User's Manual, 2015).

A detailed analysis was carried out using analytical and computational techniques to evaluate their limitations for accurate prediction of thrust and hence the yawing moment produced by the electric trimmers. However, the propeller is numerically simulated for free stream flow conditions which are not the same as those of a ducted fan. These changes require corrections to the numerical data and necessary corrections can be made by performing wind tunnel tests on a generic model of such a propeller at different tangential velocities.

ANALYTICAL METHODS

A propeller looks like a simple rotating device, but the parameters representing its performance characteristics are quite complex which can analytically be represented in terms of variables by the thrust coefficient, C_T, the power coefficient, C_p, the efficiency coefficient, η and the advance ratio, J; out of which, C_T is used in the present work to estimate thrust of a thin electric propeller, (1). Whereas, J is defined as the ratio of velocity and product of n and D.

$$C_T = \frac{T}{\rho . n^2 . D^4} \tag{1}$$

In this equation, T, ρ, n and D represent the thrust, density, number of revolutions per minute and disc diameter, respectively. In order to estimate T, different propeller theories are available in open literature, some are discussed here briefly especially their pros and cons.

Momentum Theory

Rankine-Froude were among the first who proposed a theory for the prediction of propeller performance parameters (Madsen, 1996). As per this theory, "*the propeller is assumed to be working in ideal fluid and is able to absorb all the power from the engine and later on dissipate this power by causing a pressure jump in the fluid flowing through the propeller"* (Madsen, 1996). Unfortunately, by applying this theory, the actual performance of the propeller is still a question mark, as such kind of assumption does not take into account the actual geometric profile of the propeller and viscosity of the fluids. Hence, its usage for the estimation of maximum efficiency of the propeller is quite limited.

Blade Element Method

William Froude in 1878 further refined the Rankine-Froude's Momentum theory addressing its deficiencies (Friedrich & Robertson, 2014). He proposed the idea that if we divide the blade of the propeller in such a way that every element strip can be represented by its own width and chord, then torque/force produced by each such element can be integrated to define the aerodynamic properties of the blade of a thin propeller. The limitation of the linear blade angle is that it does not account for the effect of induced velocity. For example, in the case of a helicopter, the induced velocity due to rotor disk cannot be handled by Blade Element Method.

Combined Blade Element Momentum Theory:

Glauert (1926) who first propounded this theory of Combined Blade Element Momentum, which is the combination of above mentioned two theories in which the thrust generated by the individual annulus segments can be estimated by using (2):

$$dT = 4a'(1-a)\rho U_1 \Omega r^3 \pi\, dr \tag{2}$$

Where, radius r and width dr represent the local geometric parameters, U_1, a' and Ω are free stream velocity, angular induction factor and angular velocity respectively. It is well known that the vortices are rolled up on the tip of a blade and the tip chord of the wing. This is an unavoidable phenomenon due to which there is always a decrease in lift at the tip section and increase in drag, commonly known as induced drag. Unfortunately, this theory assumes that all the elements of the blades are lift producing and it does not cater for the effect of loss in lift in the tip region. Furthermore, there is no term to account for the swirl caused by the tangential forces applied by the rotor on the flow media, whether it is liquid or gas. Since this technique is already employed by *Motocalc*® software, therefore, without going into lengthy calculations, results obtained from this open source software are used for calculating thrust.

RESULTS AND DISCUSSION

The available disc area for the propellers of electric trimmers is shown in Figure 1. The length of the model of vehicle under discussion is 4.2 m and the maximum diameter of its hull is 1.6 m. Space available for trimmers on the vertical tail is quite limited and a propeller of less than one foot as maximum disc diameter can easily be fitted without any additional structural reinforcement. Complete details of the geometric and performance parameters of the configuration are defined by Farhana (2012). *Motocalc*® is used for estimation of power and performance parameters. The graph shown in Figure 2 indicates the input load power for varying combinations of propeller pitch and diameter. All these propellers have a diameter less than one foot and operate at low Reynolds numbers (ranging between 50,000 and 100,000) due to shorter chord length (Propeller, 2015). Figure 2 shows that for a single motor, an 8 inch prop consumes lowest power and hence gives lowest thrust. On the contrary, an 11 inch propeller requires highest power while 9 inch propeller gives a middle of the road solution. Therefore, by the end of analysis, the propeller choice finally converges to a 9 inch propeller. It is also obvious from Figure 2 that 9×6 inch propeller (having slightly higher pitch) also produces an increment in the input power and hence larger thrust compared to that produced by a 9×4 inch propeller. However, a *9×4 inch* propeller was not available in the market and a *9×4.5* inch propeller is the closest to the desired specifications and hence selected for further analysis.

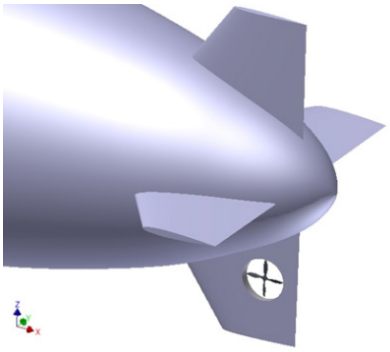

Figure 1. Location of electric trimmer on the vertical tail of the HBAV (Haque,et al., 2014)

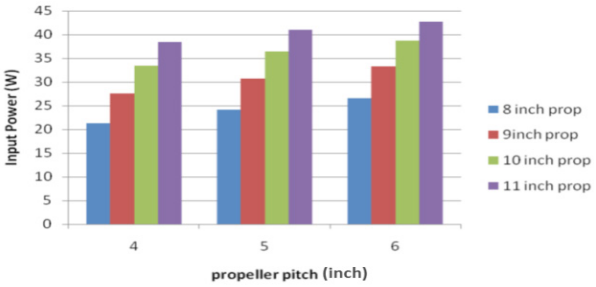

Figure 2. Input Power vs propeller pitch for different propellers

GEOMETRY DESCRIPTION

The APC propeller used in this research is described in the manual of *APC* propellers (User's Manual, 2015). Its geometry is defined in terms of diameter and pitch. It is conventional to define the diameter as twice of the radius of the circle which is swept by the tips of the blade. However, in the case of two-bladed propellers, it is the length from tip of one blade to the other blade, the value of which is 9 inch in present case. For the estimation of the yaw force, complete geometry of the selected propeller is defined by two different airfoils, NACA4412 or Clark Y airfoil, (Database of Airfoils, 2015). Both of these airfoils are initially used to evaluate the lift and drag characteristics. For the stability analysis, all the moments are computed, namely the centre of gravity *(CG)*, the location of which for our model is shown in Figure 3. The spanwise sectional views of the selected propeller are shown in Figure 4. Nomenclature used to define the geometry of the individual section of the blade, in terms of the chord and twist, is mentioned in Figure A-1 of the Appendix. The analytical results of *Motocalc* at different *RPMs* (Revolution per Minute) are also highlighted in the Appendix.

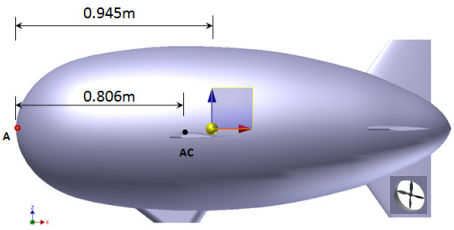

Figure 3. Location of the *CG* of the model

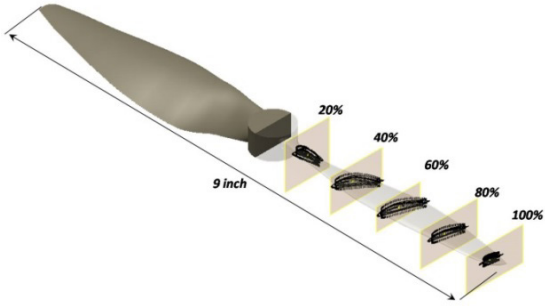

Figure 4. Sectional views of airfoil of *9 × 4.5 inch* propeller

ANALYTICAL RESULTS

Detailed geometric parameters of a *9×4.5* inch *APC* propeller have been generated in CAD and the same profile has been built in the *Motocalc* for calculating the performance parameters. The digit 4.5 in the nomenclature of the propeller represents the theoretical advancement of propeller in one revolution. Aerodynamic coefficients of the airfoils (*NACA 4412 and Clark Y* airfoil) of propeller have been estimated by using *Java-Foil*; an open source panel method, against the range of Reynolds number which have been calculated using the blade width and the resulting velocity at 75% of its radius. Plots of results taken from this software are shown in Figure 5. Combined Blade Element Momentum *(BEM)* theory is used by *Motocalc*, as the theoretical tool for the estimation of the thrust produced by the propeller. However, the accuracy of the thrust obtained by using BEM is dependent on how accurate the data points of the airfoil geometry of blade is. For the estimation of thrust force, few assumptions are made by the software. First, the airfoil has constant lift curve slope, $a_0 = 3.6897$ rad^{-1} (based on *NACA4412* C_l vs α curve) is taken as constant. Second, distribution of blade angle is linear and that the blade has negligible contribution towards its thrust in the region which is in the close vicinity of the hub of the propeller ($r < 0.012m$).

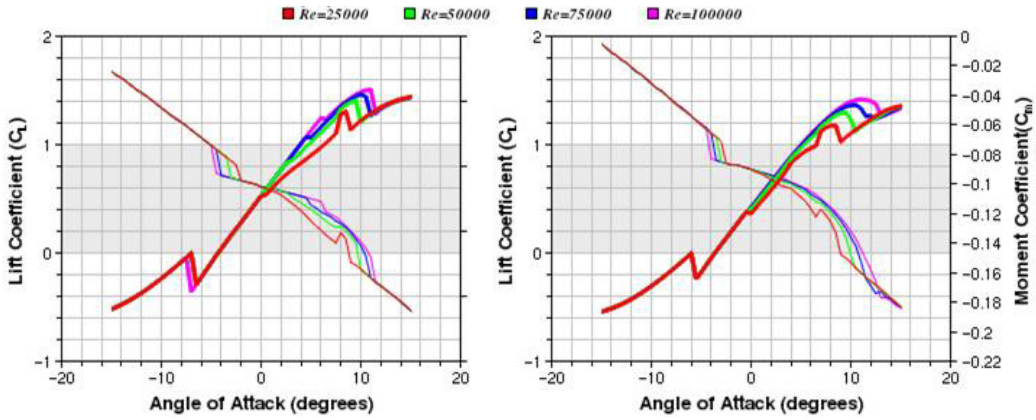

(a) NACA 4412 (b) Clark Y

Figure 5. Aerodynamic coefficients of selected airfoils obtained by *Java-Foil* at different Reynolds numbers

The contribution of each blade element for thrust is estimated by *Motocalc*® and the values obtained are integrated to get the total thrust value of the propeller. Performance parameters are then evaluated at different *RPMs* and all the results are presented in Appendix-A for quick reference. Based on these results shown in Figure A-2 to A-4, the value of η is found to be maximum at selected *RPM* for advance ratio equal to 0.36. It is also observed that with the increase in *RPMs,* there is an increase in C_P, C_T and η for lower range of J. However, this increase is not obvious for $J < 0.2$ as well as for $J > 0.46$. Against a fixed maximum *RPM* of 6900 with free stream velocity equal to 12 m/sec and Re (based on 75% of radius) equal to 8.114×10^4, total thrust is equal to 1.5974 N and 1.5926 N for *Clark Y and NACA 4412* airfoil respectively. Hence, no significant difference between *Motocalc*® results has been found for Clark Y airfoil and for NACA 4412 airfoil.

COMPUTATIONAL RESULTS AND ITS COMPARISON

The *CFD* analysis is carried out using commercial *CFD* software *Fluent*® to capture key flow physics in the propeller's aerodynamic characteristics. First, the geometry (Figure 6(a)) is created based on available information about the geometrical parameters and unstructured sliding mesh is employed. Such a grid allows adjacent grid to slide over it. Special attention is paid to get more grid resolution close to the wall Figure 6(b). Farfield boundary condition was applied for the computational domain shown in Figure 6(c) and the required *RPM* is incorporated in the moving boundary condition of the wall of propeller. The *SA* turbulence model was used in this research. Unsteady simulation with dual-time marching is also carried out to get a numerical solution in the form of pressure distribution on the windward and leeward side of the propeller, which finally provides its thrust value from the said pressure difference. Reynolds number and free stream velocity are kept the same as that used in the analytical work for combined BEM theory. Streamline plots show the roll-up path lines at the tip of the propeller as seen in Figure 6(d) and they show that there will be additional induced drag as well as tip loss in thrust.

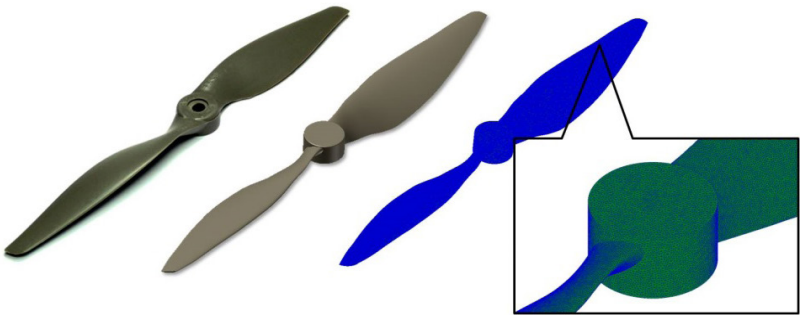

(a) Existing Propeller and its CAD Model (b) Surface Mesh

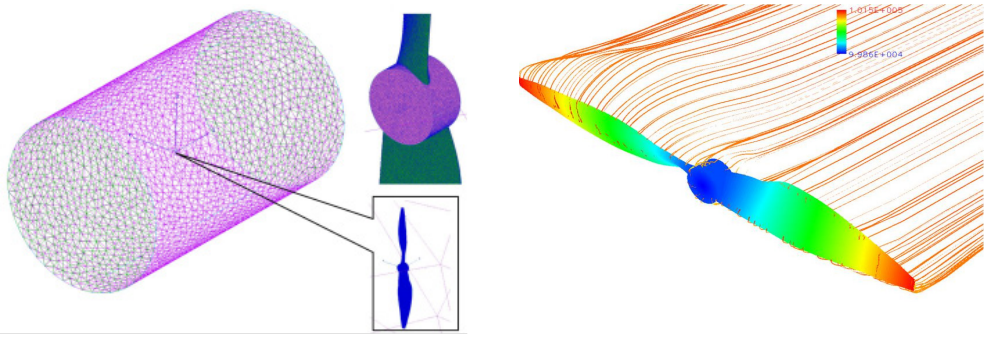

(c) Computational Domain (d) Streamlines with contours of pressure

Figure 6. CFD Analysis at R_e (based on 75% of radius) = 8.11 × 10^4, V = 12 *m/s* at sea level condition

However, the computed results of *9×4.5* inch propeller have given thrust value equal to *1.89 N* and thus over-prediction is shown by *CFD* work compared to the analytical value of *1.59 N*. This over-prediction by *Motocalc* is mainly due to the limitation of combined Blade Element Momentum theory as described earlier. The thrust produced by the propeller interacts

with the tangential free stream velocity causing an obvious loss of yaw force. It is roughly assumed that *33 %* loss is expected which will result in a yaw force of *1.27 N* and the moment produced around the fixed location of the *CG* will be equal to *3.81 N.m*. This assumption might be open to question but it will give a starting point for the preliminary lateral stability analysis.

Electric trimmers studied in this work can generate thrust force in the opposite direction as well. For this purpose, the pilot has to first stop the motor for negative yaw. This additional fatigue on the operator can be minimised by employing more electric motors at the front part of the hybrid airship, pictorially shown in Figure 7.

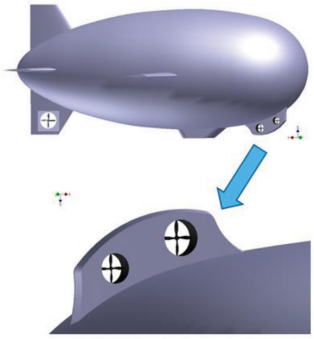

Figure 7. Twin electric motors at the nose of the hull

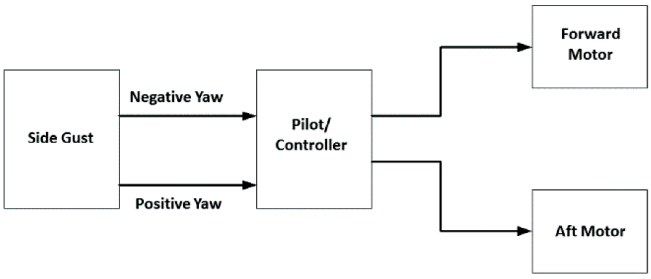

Figure 8. Block diagram for differential thrust

In the case of the electric motor failure, an alternative yaw source for the system can be introduced. For such twin electric motors, yaw is controlled by creating difference in the speed of motors i.e. difference in *revolution per minute (RPM)* of the forward and the aft fan. This is described in Figure 8 with the help of a block diagram. Speed of motors of each group can be controlled by the pilot. If no yaw manoeuvring is required, both the outputs are driven with the same pulse width signal in order to keep uniform motor speed, but in opposite direction. This concept needs thorough calculations for different flight conditions which is not covered in this study.

CONCLUSION

Based on the analytical approach, it has been found that a *9×6* inch propeller (having slightly higher pitch) produces a minute increment in the value of static as well as forward thrust, when compared with a *9×4.5* inch propeller. First order approximation of thrust produced by the propeller can be done by using *Motocalc* for which complete geometric details of the propeller and the flow conditions are a prerequisite for analysis. However, *Motocalc* cannot capture the effect of wake separation and tip losses. A first order approximation of the control force and moment generated by the electric trimmers for full load and free stream condition can be done from the *CFD* analysis. The *CFD* results can also be utilised for the dynamic stability analysis of such aerial vehicles.

ACKNOWLEDGEMENTS

The authors would like to acknowledge the support of the Ministry of Science, Technology and Innovation (MOSTI), Malaysia, under the grant 06-01-08-SF0189 for this research work.

REFERENCES

Airfoils. (2015). *Database of Airfoils*. Retrieved September, 2105, from http://www. *airfoiltools.com*

Andan, A. D., Asrar, W., & Omar, A. A. (2012). Investigation of Aerodynamic Parameters of a Hybrid Airship. *Journal of Aircraft*, *49*(2), 658–662.

Brandt, J. B. (2005). *Small-Scale Propeller Performance at Low Speeds*. (Master dissertation). Department of Aerospace Engineering, University of Illinois at Urbana-Champaign, Illinois.

Carichner, G. E. & Nicolai, L. M. (2013). *Fundamentals of Aircraft and Airship Design: Volume II, Airship Design*. (J. A. Schetz, Ed.). American Institute of Aeronautics and Astronautics, AIAA.

Friedrich, C., & Robertson, P. A. (2014). Hybrid-electric propulsion for aircraft. *Journal of Aircraft, 52*(1), 176-189.

Farhana, A. (2012). *The development of a mathematical model of a hybrid airship*. (Master dissertation). University of Southern California, USA.

Glauert, H. (1926). *The elements of aerofoil and airscrew theory*. Cambridge University Press, UK.

Haque, A. U., Asrar, W., Omar, A. A., Sulaeman, E., & Ali, J. S. M. (2014). Static longitudinal stability of a hybrid airship. In *Proceedings of 2014 11th International Bhurban Conference on Applied Sciences & Technology (IBCAST) Islamabad, Pakistan*, (pp.343–348). doi:10.1109/IBCAST.2014.6778167.

Khoury, G. A., & Gillett, J. D. (1999). *Airship Technology*. New York, NY: Cambridge Univ. Press.

Madsen, H. A. (1996 Dec). A CFD analysis for the actuator disc flow compared with momentum theory results". In *Proceedings of the 10th IEA Symposium of Aerodynamics and Wind Turbines*. Edinburgh, UK.

Propeller, A. P. C. (2012). *APC Propeller Performance Data*. Retrieved September, 2105, from https://www.apcprop.com/Articles.asp

Schroijen, M. J. T., Veldhuis, L. L. M., & Singerland, R. (2008). Propeller slipstream investigation using the Fokker F27 wind tunnel model with flaps deflected. In *26th International Congress of the Aeronautical Sciences, ICAS-2008*.

Stockbridge, C., Ceruti, A., & Marzocca, P. (2012). Airship Research and Development in the Areas of Design, Structures, Dynamics and Energy Systems. *International Journal of Aeronautical and Space Sciences*, *13*(2), 170–187. doi:10.5139/IJASS.2012.13.2.170

User's Manual. (2015). *MotoCalc Electric Flight Performance Prediction Software*. Retrieved July, 2015, from www.motocalc.com/

Zeune, C. O. M., & Logan, M. (2008, August). Analytical–Experimental Comparison for Small Electric Unmanned Air Vehicle Propellers. In *26th AIAA Applied Aerodynamics Conference*, (pp. 18-21).

APPENDIX

All the nomenclatures used to define the geometry in terms of the individual sections of the selected *APC* propeller are shown in Figure A-1. All the necessary calculations have been done by *Motocalc* to estimate the performance parameters of the propeller, Figure A-2 to Figure A-4. User limitations of this software are found in the User's Manual (2015). The results obtained delineate uniform trends as there is no scattering of data at different *RPM*. All these analytical results are obtained using the aerodynamic data of NACA 4412 airfoil as sectional profile of the blade. It can be observed from the figures an increase in *RPM* corresponds with an increase in C_P, C_T and η for lower range of J.

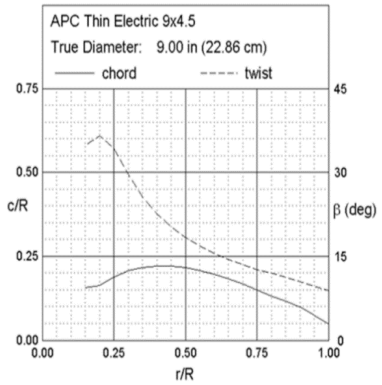

Figure A-1. Geometric parameters of the selected propeller

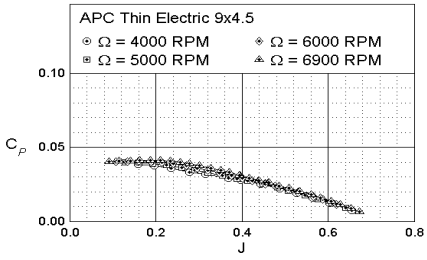

Figure A-2. Variation in C_P with J for different *RPM*

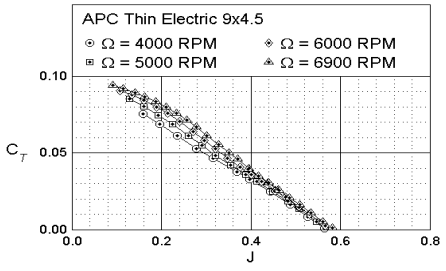

Figure A-3. Variation in C_T with J

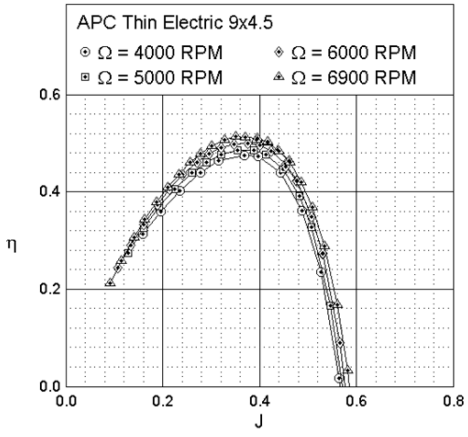

Figure A-4. Variation in η with J

However, this increase is not obvious for $J < 0.2$ as well as for $J > 0.46$. These analytical results are limited for small propellers and due to their structural anatomy, their performance results cannot be used for their larger counterparts. Moreover, similar to other thin electric propellers (Brandt, 2005; Zeune, & Logan, 2008), wind tunnel testing is recommended to investigate further the performance parameters, especially when the fan is ducted at the tail of the HBAV. For example, with the help of torque transducers, the trend plot of C_P at different RPMs can obtained.